Lawrence Berkeley National Laboratory
Recent Work

Title
Self-Diffusion and Relative Diffusion in Defect Turbulence

Permalink
https://escholarship.org/uc/item/9w41m53m

Journal
Physica D, 96(1/4/2008)

Authors
Huber, G.
Schroeder, E.
Alstrom, P.

Publication Date
1995-03-01

eScholarship.org Powered by the California Digital Library
University of California

LBL-36285
UC-405
Preprint

Lawrence Berkeley Laboratory

UNIVERSITY OF CALIFORNIA

Physics Division

Mathematics Department

To be submitted for publication

Self-Diffusion and Relative Diffusion in Defect Turbulence

G. Huber, E. Schröder, P. Alstrøm

March 1995

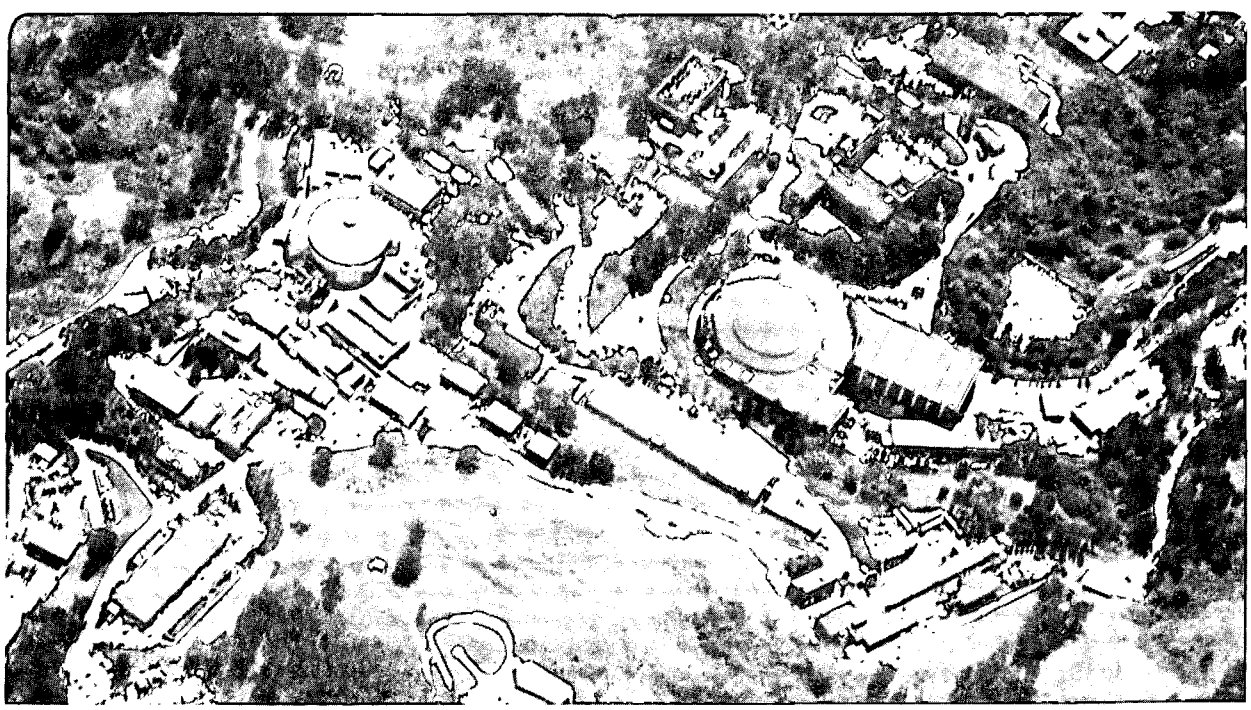

REFERENCE COPY
Does Not
Circulate
Bldg. 50 Library.
Copy 1
LBL-36285

Prepared for the U.S. Department of Energy under Contract Number DE-AC03-76SF00098

DISCLAIMER

This document was prepared as an account of work sponsored by the United States Government. While this document is believed to contain correct information, neither the United States Government nor any agency thereof, nor the Regents of the University of California, nor any of their employees, makes any warranty, express or implied, or assumes any legal responsibility for the accuracy, completeness, or usefulness of any information, apparatus, product, or process disclosed, or represents that its use would not infringe privately owned rights. Reference herein to any specific commercial product, process, or service by its trade name, trademark, manufacturer, or otherwise, does not necessarily constitute or imply its endorsement, recommendation, or favoring by the United States Government or any agency thereof, or the Regents of the University of California. The views and opinions of authors expressed herein do not necessarily state or reflect those of the United States Government or any agency thereof or the Regents of the University of California.

LBL-36285

SELF-DIFFUSION AND RELATIVE DIFFUSION IN DEFECT TURBULENCE*

Greg Huber[1,2], Elsebeth Schröder[2], and Preben Alstrøm[2]

[1]Department of Mathematics and Lawrence Berkeley Laboratory
University of California, Berkeley, CA 94720, USA
[2]Center for Chaos and Turbulence Studies, Niels Bohr Institute
Blegdamsvej 17, DK-2100 Copenhagen Ø, Denmark

March 1995

* This work was supported in part by the Applied Mathematical Sciences Subprogram of the Office of Energy Research, U.S. Department of Energy under Contract DE-AC03-76SF00098.

Self-Diffusion and Relative Diffusion in Defect Turbulence

Greg Huber[1,2], Elsebeth Schröder[2], and Preben Alstrøm[2]

[1] *Department of Mathematics and Lawrence Berkeley Laboratory*
University of California, Berkeley, CA 94720, USA
[2] *Center for Chaos and Turbulence Studies, Niels Bohr Institute*
Blegdamsvej 17, DK-2100 Copenhagen Ø, Denmark

Abstract

We consider the motion of particles and scalar flow in the defect-turbulent regime of the complex Ginzburg-Landau field. We find that the particle motion is diffusion-like at large time scales, whereas the motion is dominated by trapping of particles by defects of the field at short time scales. Consequently the diffusion constant is constrained. For relative motion of two particles we find that at a relative distance s the distribution of ds^2/dt is exponential rather than Gaussian as would be the case for Brownian motion.

Particles are kicked around in a turbulent flow like helium balloons in a hurricane [1]. Their complicated and unpredictable individual and relative motion differ from the Brownian ideal in important ways and present a host of outstanding problems [1, 2, 3, 4, 5]. Likewise, the related issue of a turbulently-advected passive scalar presents its own analytical difficulties [6, 7, 8]. The class of turbulence studied here, defect turbulence, occurs in spatially-extended systems near the threshold of a Hopf bifurcation [9, 10]. In two dimensions, it is characterized by the motion, creation and annihilation of point defects (vortices).

We have undertaken a study of particle motion in the background of defect turbulence. We use the complex Ginzburg-Landau equation,

$$\partial_t A(\boldsymbol{x},t) = A(\boldsymbol{x},t) - (1+i\alpha)|A(\boldsymbol{x},t)|^2 A(\boldsymbol{x},t) + (1+i\beta)\nabla^2 A(\boldsymbol{x},t), \qquad (1)$$

for the dynamics of the underlying (complex) amplitude field $A(\boldsymbol{x},t)$. Here α and β are real numbers, and we take $A = Re^{i\phi}$. Of crucial importance are the defects of the phase field, i.e. the singularities of $\phi(\boldsymbol{x},t)$, where the modulus is identically zero: $R(\boldsymbol{x},t) = 0$. Depending on the values of α and β (Fig. 1), the vortices either appear in a frozen state, where spiral waves in the phase $\phi(\boldsymbol{x},t)$ wind

around fixed vortex cores, or in a turbulent state where the vortices move rapidly and are annihilated and created in vortex-antivortex pairs [10, 11, 12, 13]. The vortices are characterized by their vorticity. The phase gradient points towards the vortex core, except in the area close to the core. There, the gradient lines spiral around the core counterclockwise for vortices of positive vorticity, and clockwise for negative vorticity.

The particle is given a velocity

$$\boldsymbol{v} = \frac{\mathrm{d}\boldsymbol{r}}{\mathrm{d}t} = \Gamma \boldsymbol{\nabla} \phi(\boldsymbol{r}, t) \tag{2}$$

where $\boldsymbol{r}(t)$ is the particle position, and the coefficient Γ is treated as an adjustable parameter (which can be positive or negative). The particle has no inertia in this scheme, the equation of motion being purely dissipative. We are interested in the trajectory and the statistics of particle motion when the underlying field is turbulent. However, for the purposes of illustration, we first consider the particle in the frozen state, where the influence of the defects is clearly discerned and understood.

Eqs. (1) and (2) were discretized using the coupled-map approximation discussed in [11]. We used a 128×128-lattice with periodic boundary conditions, and random initial conditions (A is random within the unit circle). In all cases, we let the system achieve a steady-state vortex density before recording data. The phase gradient at the (off-lattice) particle position $\boldsymbol{r}$ in Eq. (2) was interpolated from four first-order phase gradients at the four nearest lattice sites.

The motion of the particle in the field of one or a few vortices is the basis by which we understand the more complicated particle motions in the turbulent case. It follows from the choice of the equation of motion (2) that the particle is attracted to the vortices when Γ is positive, and repelled by them when Γ is negative. In the frozen vortex state, the particle will either spiral into a vortex and be trapped, or it will follow the domain walls separating the spiral waves until it gets stuck at a junction of three domain walls. In our numerical simulations on a lattice, the spiraling motion into a vortex is eventually replaced by a circulating motion around the vortex core. The phase gradient diverges in the center of the vortex, so in a continuum, the particle velocity keeps increasing. This (unphysical) divergence can be removed by multiplying the right hand side of Eq. (2) by $|A|$ or $|A|^2$.

In the turbulent regime, and for Γ positive, the particle is still attracted to the vortices and tries to move with them. The lifetime of a vortex in the turbulent field is finite, however, so the particle will eventually be abandoned and must then find and stick to another vortex. The amount of time the particle spends near a vortex increases with the absolute value of Γ, since increasing $|\Gamma|$ means increasing the velocity of the particle, thereby enabling it to follow the motion of the vortex for a longer period of time. When Γ is sufficiently large, the particle is trapped by the vortex until the vortex undergoes annihilation.

Figures 2a and 2b show the traces of a particle moving at $\Gamma = 1$ and $\Gamma = 10$. We used $\alpha = 1$ and $\beta = -2$ (open circle in Fig. 1). Complete trapping is observed for $\Gamma = 10$. For negative Γ, the particle is repelled by the vortices, so no trapping is observed (Fig. 2c).

The intriguing combination of vortex pinning and the motion between the vortices is even more emphasized when plotting the time variation of the "energy" $\epsilon \equiv \boldsymbol{v}^2$. This is shown in Fig. 3, revealing a very intermittent behavior. As seen, ϵ is large while the particle is trapped by a vortex, indicating that the phase gradients close to the vortices are large. When the particle moves between vortices, ϵ decreases drastically to a small value.

To study self-diffusion, we consider the mean square displacement $< \Delta r^2 >$ of the particle as a function of the time interval Δt. In Fig. 4a $< \Delta r^2 >$ is plotted versus Δt on double-logarithmic scale for $\Gamma = 1,\ 10,\ 100$. The inset shows a longer run for $\Gamma = -1.2$. At low Δt we find that the motion is ballistic, $< \Delta r^2 > \propto (\Delta t)^2$, while at large time intervals the motion seems to approach normal diffusion, $< \Delta r^2 > = D\Delta t$ where D is the self-diffusion constant.

Figure 4b shows the diffusion constant D obtained as a function of Γ. When $|\Gamma| << 1$, we find that $D \propto \Gamma^2$. The appropriate physical picture in this case is that of a particle being kicked about by an underlying random vector field. In this picture, a squared displacement of $< \Delta r^2 >$ will be proportional to Δt, with a prefactor proportional to $\Gamma^2 < |\nabla\phi|^2 >$. As the value of Γ increases, the vortex trapping of particles becomes more efficient, and a hump develops in the mean square displacement curve (Fig. 4a). Only well above the time the particle is trapped by a vortex the diffusion law is recovered. The trapping effect indicates that the self-diffusion constant eventually is limited to that of the vortex diffusion. Accordingly, at large Γ we find that the velocity of the particle is large enough to follow any motion of the vortices. Thus, it is solely the underlying field dynamics that determines the dynamics of the particle. In this case, ($|\Gamma| >> 1$), D is independent of Γ, as seen in Fig. 4b.

The motion of one particle relative to another in a turbulent field is called Richardson diffusion. If $\boldsymbol{s} \equiv \boldsymbol{r}_2 - \boldsymbol{r}_1$ denotes the position of particle 2 relative to particle 1, an important question in the field of turbulence is the dependence of $D(s) =< d\boldsymbol{s}^2/dt >$ on the distance $s = |\boldsymbol{s}|$. If $D(s)$ is constant, the relative motion is diffusion-like. In general, two advected particles will probe velocity correlations on scales of order their separation.

In order to determine $D(s)$ we follow two routes: One is the Eulerian, where two lattice points a distance s apart is selected, and at any given time two particles are launched and followed for one time step to determine $d\boldsymbol{s}^2/dt$. The other route is the Lagrangian, where two particles are launched and followed in time, sampling $d\boldsymbol{s}^2/dt$ as a function of t. From the first $D(s)$ is obtained directly, averaging over time. From the second approach, the values of $d\boldsymbol{s}^2/dt$ for various values of s has to be collected from many traces of particle pairs, or from very long traces, where the pair of particles are a distance s apart many times.

Figure 5a shows a semi-logarithmic plot of the distribution $P(D)$ for $s = 75$ and $s = 200$ obtained from the Lagrangian approach. The mean value is very small compared to the width of the distribution, so no conclusive results are obtained for the s dependence of $D(s)$. This is also the case for the Eulerian approach. However, $P(D)$ is clearly not Gaussian, as is found for Brownian motion. Rather the distributions fall off exponentially. We find that the width increases linearly with s for both the Lagrangian and the Eulerian approach (Fig. 5b).

We find when launching many particles that these in the course of time merge [14]. To illustrate the effective particle field, we comment on adding a passive scalar field to Eq. (1).

$$\partial_t \Theta + \nabla \cdot (\boldsymbol{v}\Theta) = \kappa \nabla^2 \Theta \tag{3}$$

Figure 6 shows the particle concentration in grey code. We have used a non-zero diffusivity $\kappa = 1$, and the velocity $\boldsymbol{v} = \nabla\phi$. It is clear that the concentration is not homogeneous. Rather, spikes are observed in the particle concentration corresponding to the location of the vortices. For the velocity $\boldsymbol{v} = -\nabla\phi$ the concentration is at its maximum at boundaries between the domains of the vortices.

In conclusion, we have analyzed particle motion in the two-dimensional Ginzburg-Landau field. On long time scales the motion seems to be diffusion-like. However, the trajectories are heavily constrained by trapping at vortices, which puts an upper limit on the diffusion constant. The trapping gives rise to an intermittent behavior of the energy $\propto \boldsymbol{v}^2$. We have also considered relative diffusion, and we find that the distribution of ds^2/dt for a given s is exponential rather than Gaussian as is the case for Brownian motion.

This work was supported by the Novo-Nordisk Foundation, the Danish Natural Science Research Council, and the Danish Research Academy.

References

[1] L. F. Richardson, Proc. Royal Soc. (London) A **110**, 709 (1926).

[2] F. Gifford Jr., J. Meteorology **14**, 410 (1957).

[3] H. G. E. Hentschel and I. Procaccia, Phys. Rev. A **28**, 417 (1983).

[4] R. Ramshankar, D. Berlin, and J. P. Gollub, Phys. of Fluids, A **2**, 1955 (1990).

[5] P. Alstrøm, J. S. Andersen, W. I. Goldburg, and M. T. Levinsen, Chaos, Solitons, and Fractals, to appear.

[6] R. Ramshankar and J. P. Gollub, Phys. Fluids A **3**, 1344 (1991).

[7] P. Constantin, I. Procaccia, and K. R. Sreenivasan, Phys. Rev. Lett. **67**, 1739 (1991).

[8] I. Procaccia and P. Constantin, Europhys. Lett. **22**, 689 (1993).

[9] Y. Kuramoto *Chemical Oscillations, Waves, and Turbulence* (Springer-Verlag, Berlin, 1984).

[10] P. Coullet, L. Gil, and J. Lega, Phys. Rev. Lett. **62**, 1619 (1989); L. Gil, J. Lega, and J. L. Meunier, Phys. Rev. A **41**, 1138 (1990).

[11] T. Bohr, A. W. Pedersen, M. H. Jensen, and D. A. Rand, in *New Trends in Nonlinear Dynamics and Pattern Forming Phenomena: The Geometry of Nonequilibrium,* edited by P. Coullet and P. Huerre (Plenum, New York, 1989); T. Bohr, A. W. Pedersen, and M. H. Jensen, Phys. Rev. A **42**, 3626 (1990); X.-G. Wu and R. Kapral, J. Chem. Phys. **94**, 1411 (1991).

[12] I. S. Aranson, L. Aranson, L. Kramer, and A. Weber, Phys. Rev. A **46**, R2992 (1992).

[13] G. Huber, P. Alstrøm and T. Bohr, Phys. Rev. Lett. **69**, 2480 (1992).

[14] Merging has also been observed for the one-dimensional Kuramoto-Sivanshinskii equation [T. Bohr and A. Pikovsky, Phys. Rev. Lett. **70**, 2892 (1993)].

Figure Captions

Figure 1: Phase diagram indicating frozen and turbulent state. The open circle indicates the values used in the simulations ($\alpha = 1, \beta = -2$).

Figure 2: Particle traces in the turbulent state, system size 128×128, for the parameter values (a) $\Gamma = 1$, (b) $\Gamma = 10$, (c) $\Gamma = -1$.

Figure 3: Energy $\epsilon = \boldsymbol{v}^2(t)$.

Figure 4: (a) The mean square distance $< \Delta r^2 >$ versus t for $\Gamma = 1$ (small circles), $\Gamma = 10$ (diamonds), and $\Gamma = 100$ (big circles). System size 128×128. *Inset:* $< \Delta r^2 >$ versus t for $\Gamma = -1.2$. (b) The self-diffusion coefficient D as a function of the parameter $|\Gamma|$, double-logarithmic scale. $\Gamma < 0$: triangles, $\Gamma > 0$: circles.

Figure 5: (a) Distribution $P(D)$ for the Lagrangian approach. Distances between particles are $s = 75$ (open circles) and $s = 200$ (black circles) for the parameter $\Gamma = 1$. b) Width $\sigma(s)$ of the distribution functions for the Eulerian (diamonds) and the Lagrangian approach (black circles). $\Gamma = 10$.

Figure 6: Particle concentration in grey code for the case of a passive scalar. Black is maximum. The velocity field is given by $\boldsymbol{v} = \nabla\phi$, the system size is 256×256 and the diffusivity is $\kappa = 1$.

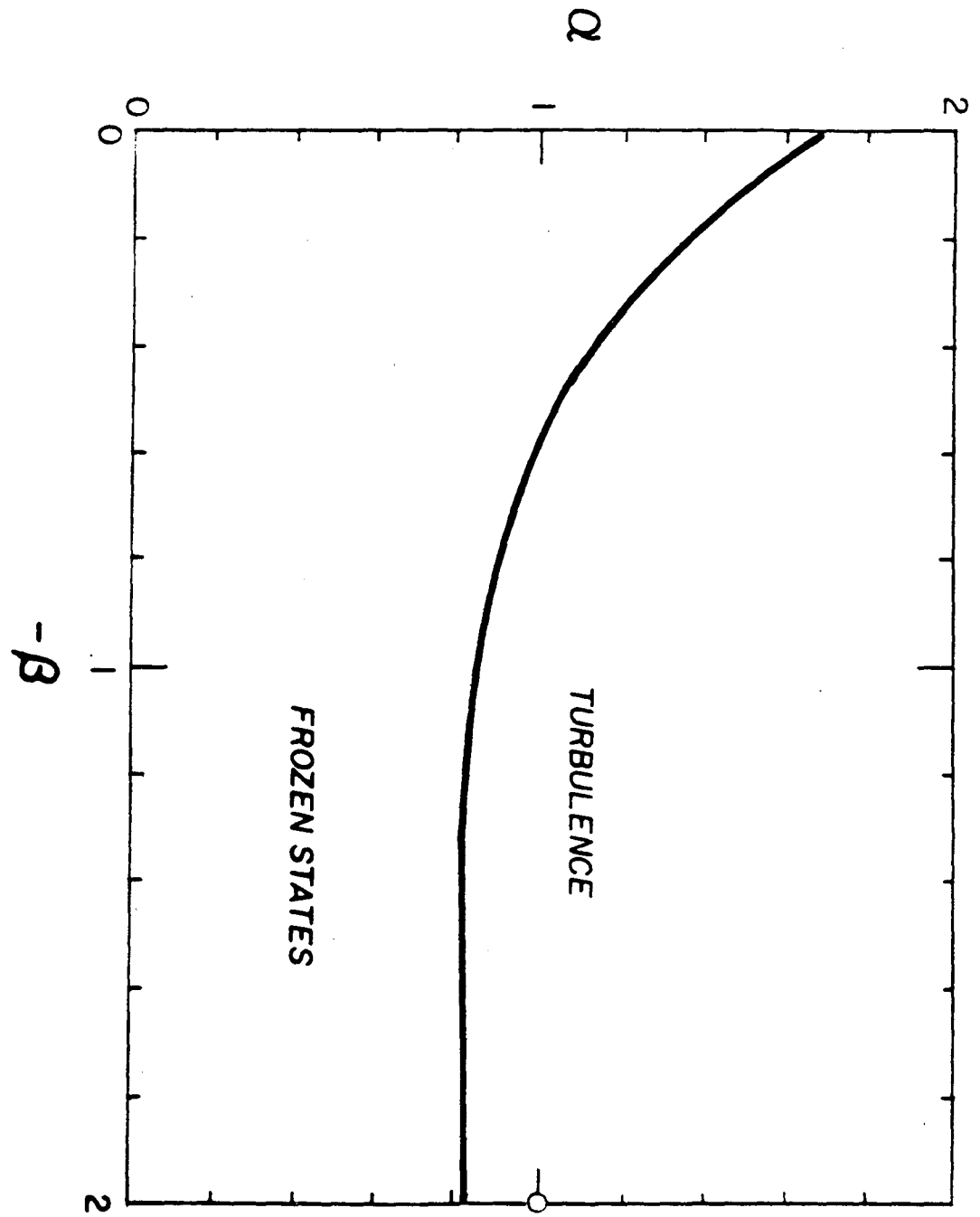

Fig. 1

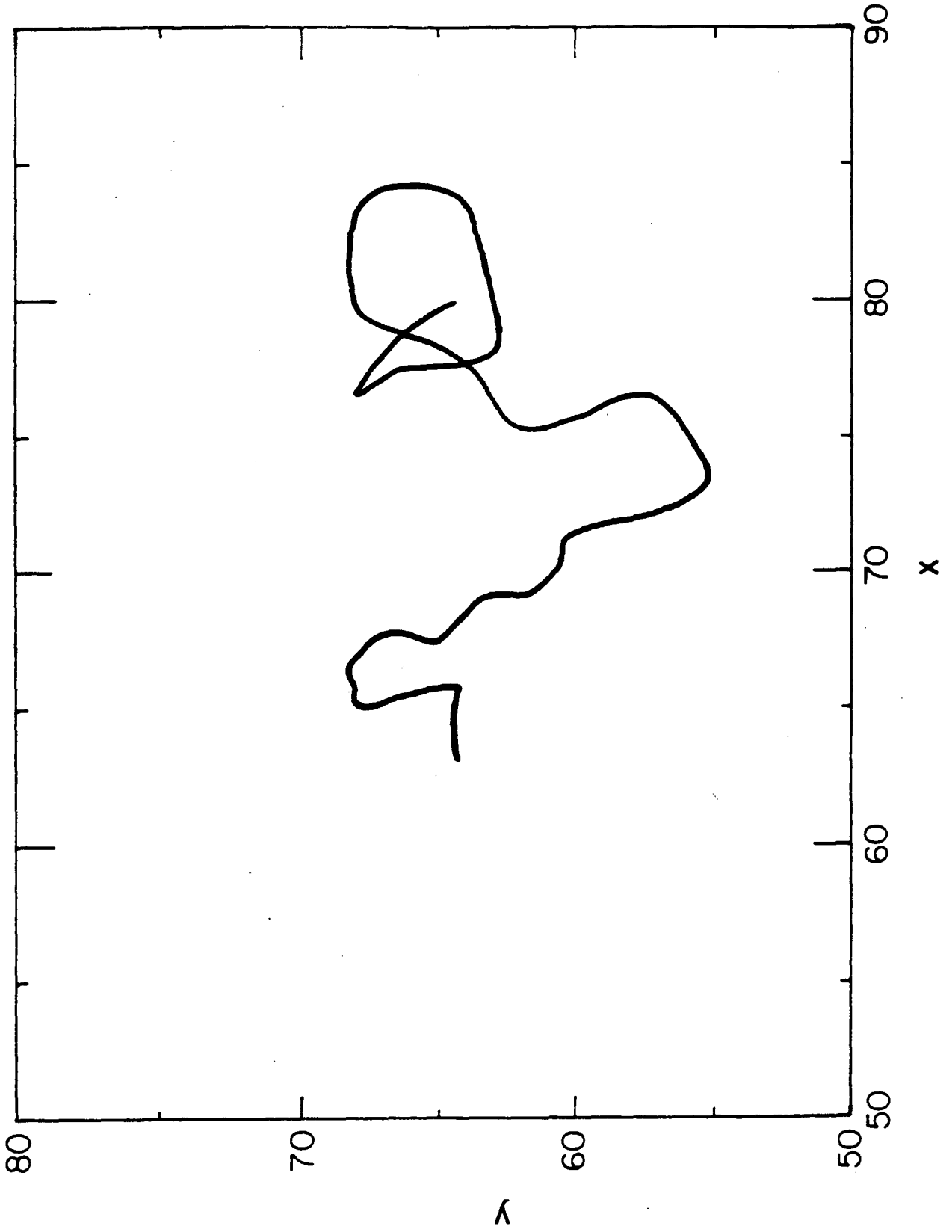

Fig. 2a

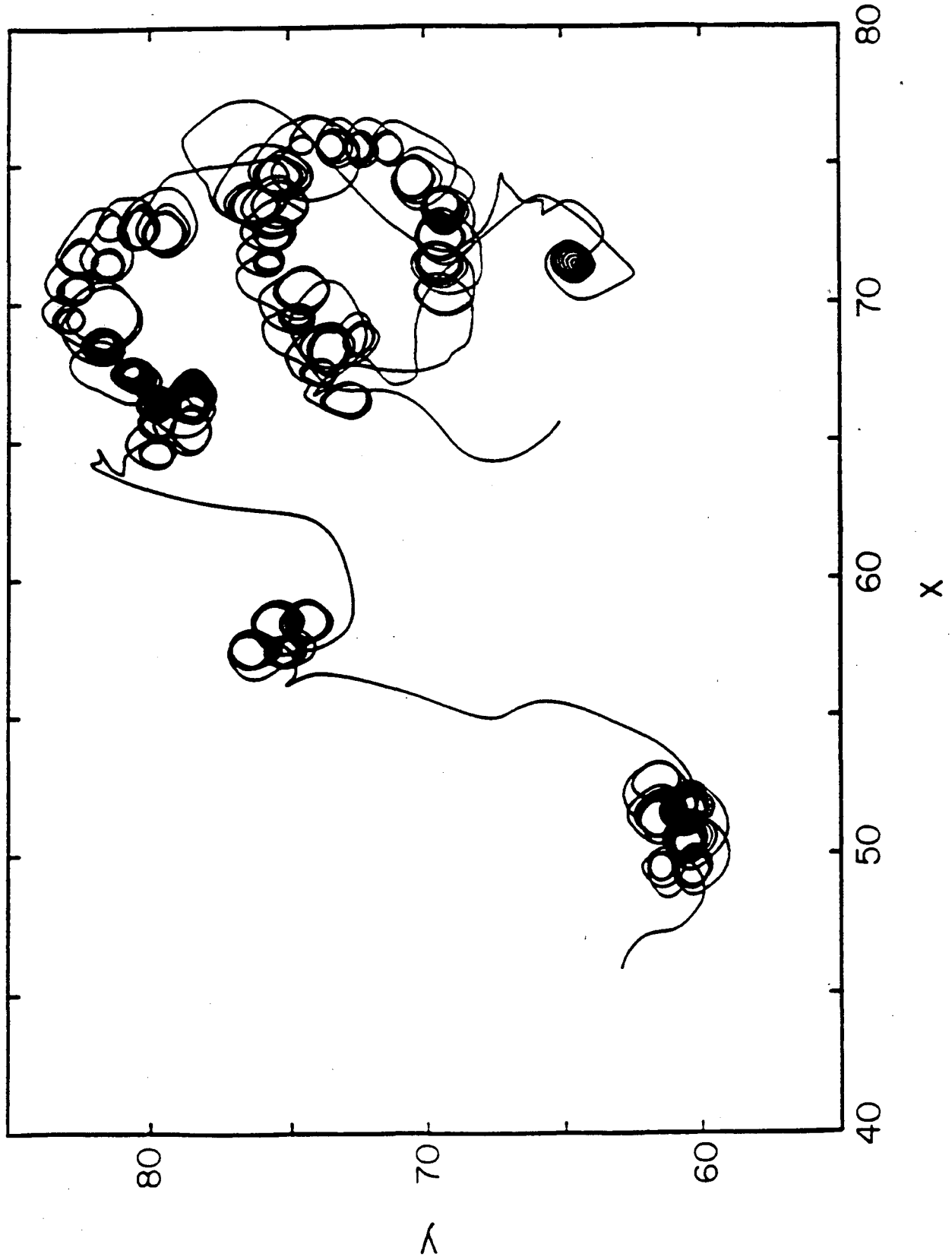

Fig. 2b

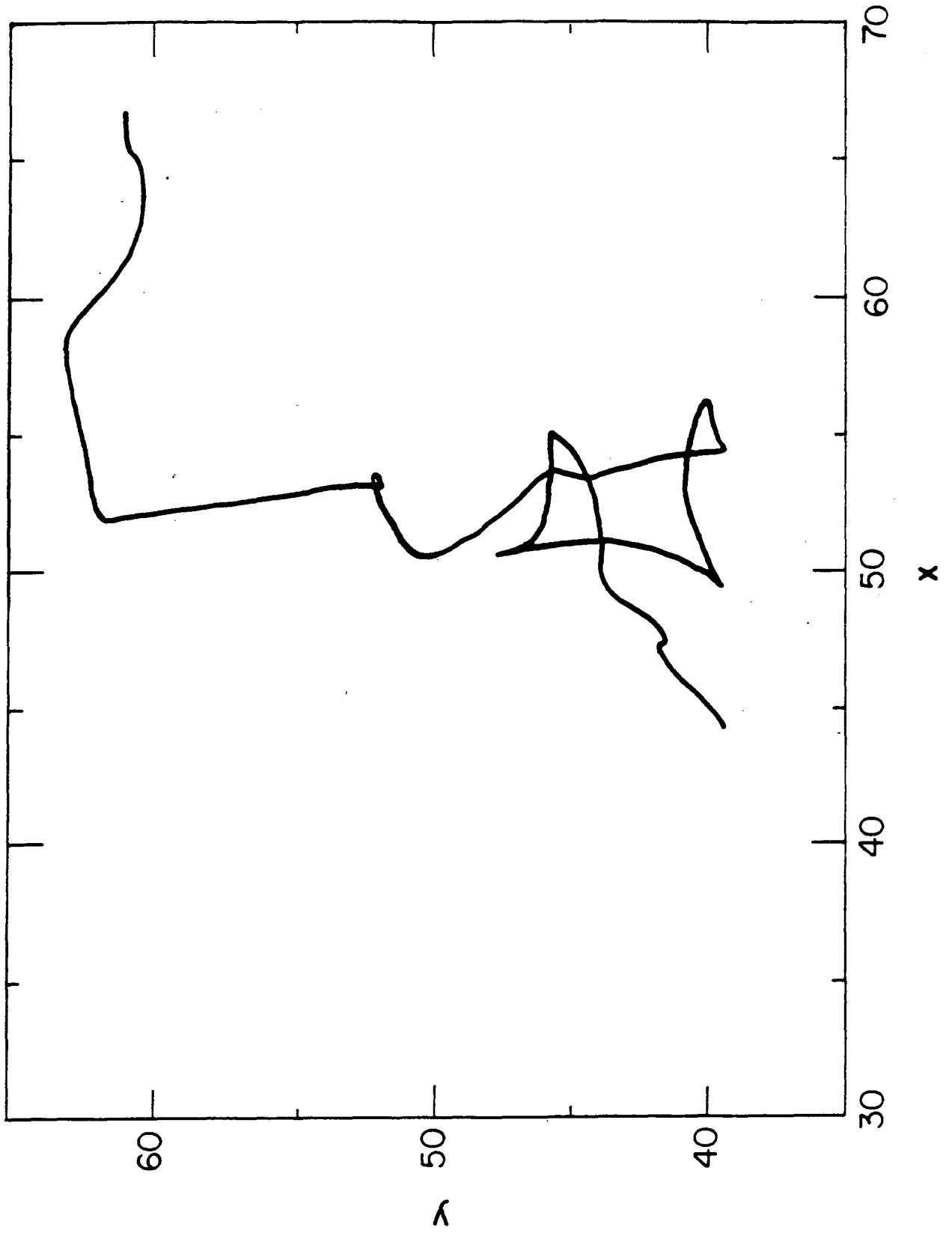

Fig. 2c

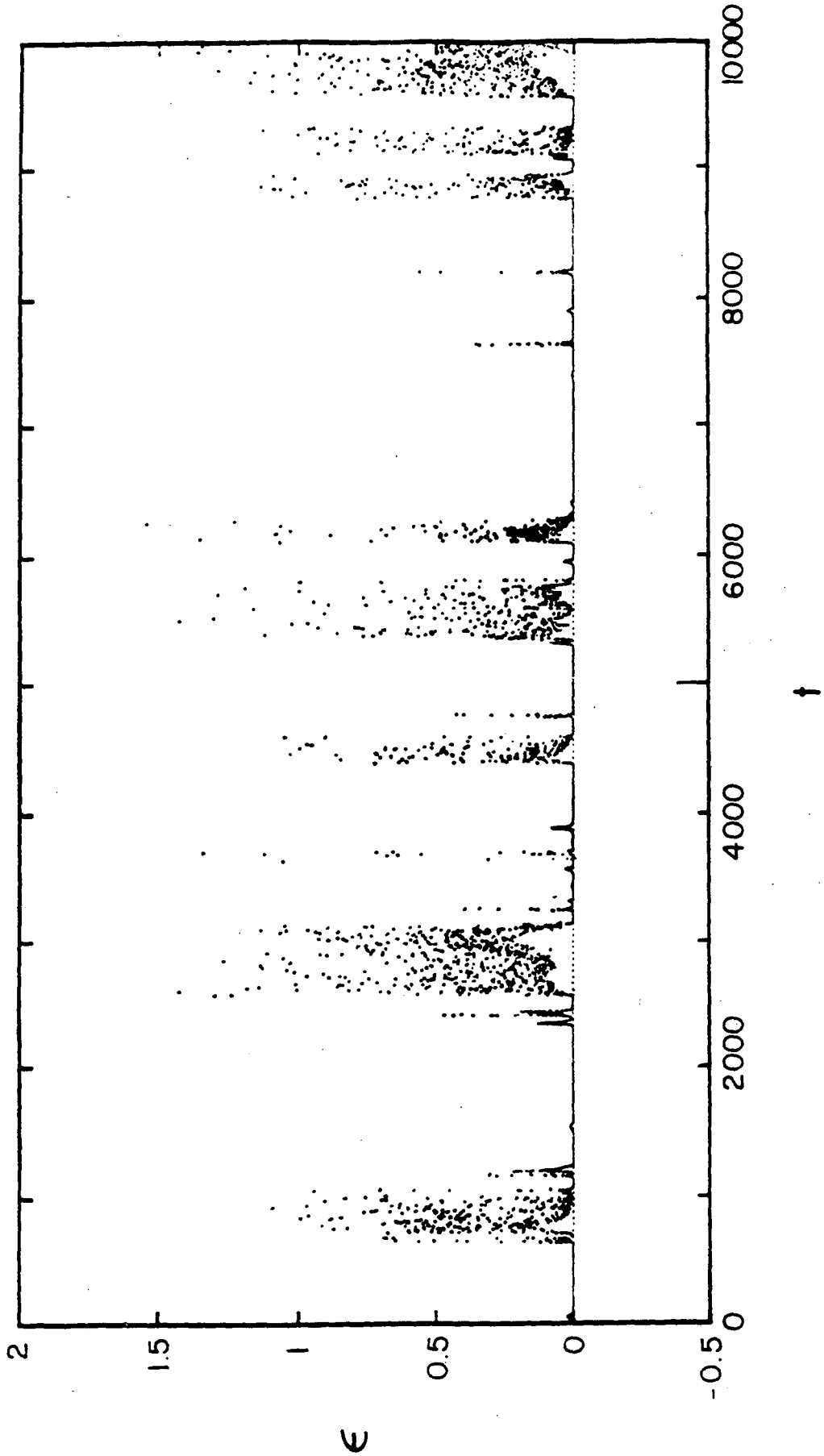

Fig. 3

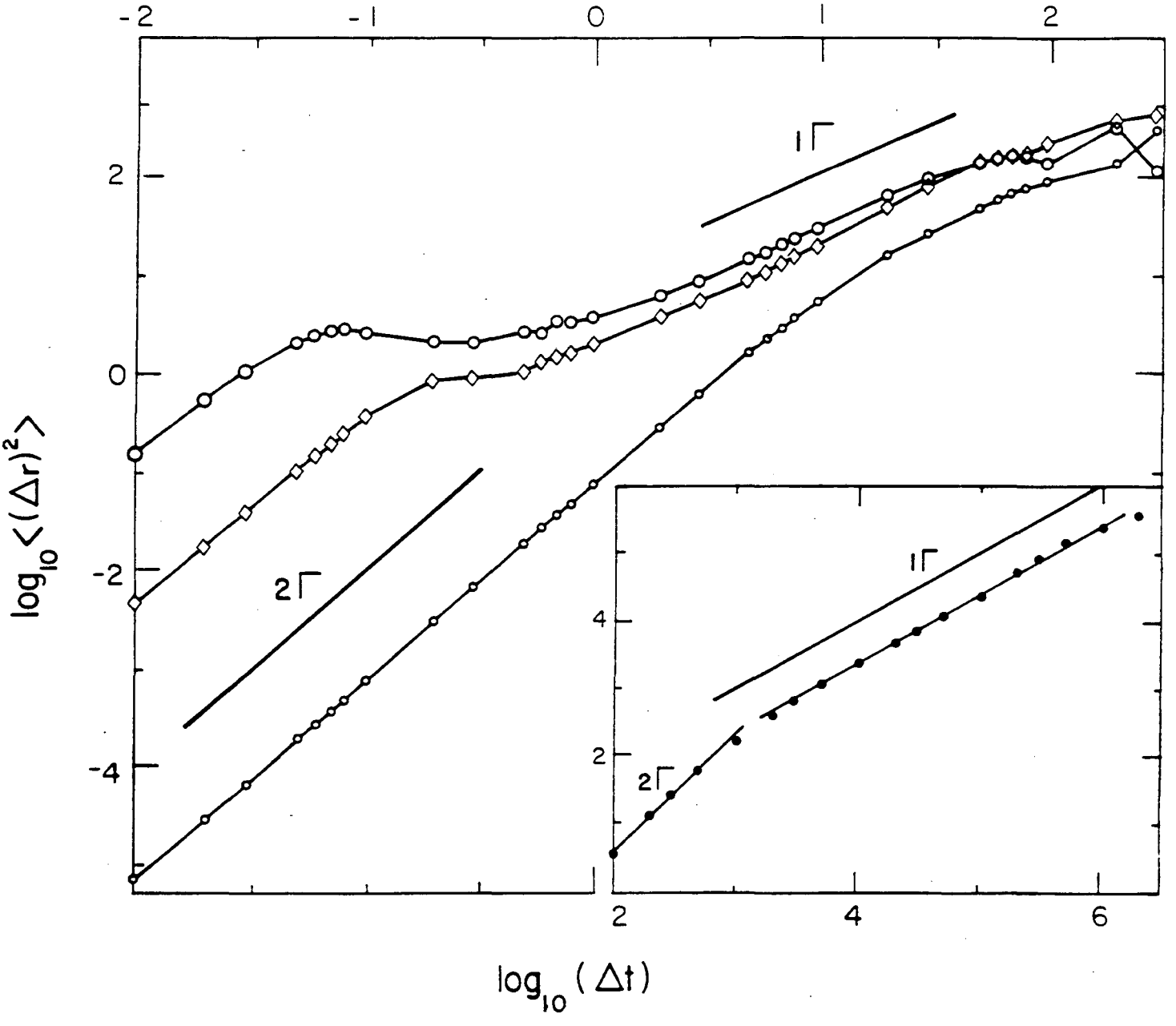

Fig. 4a

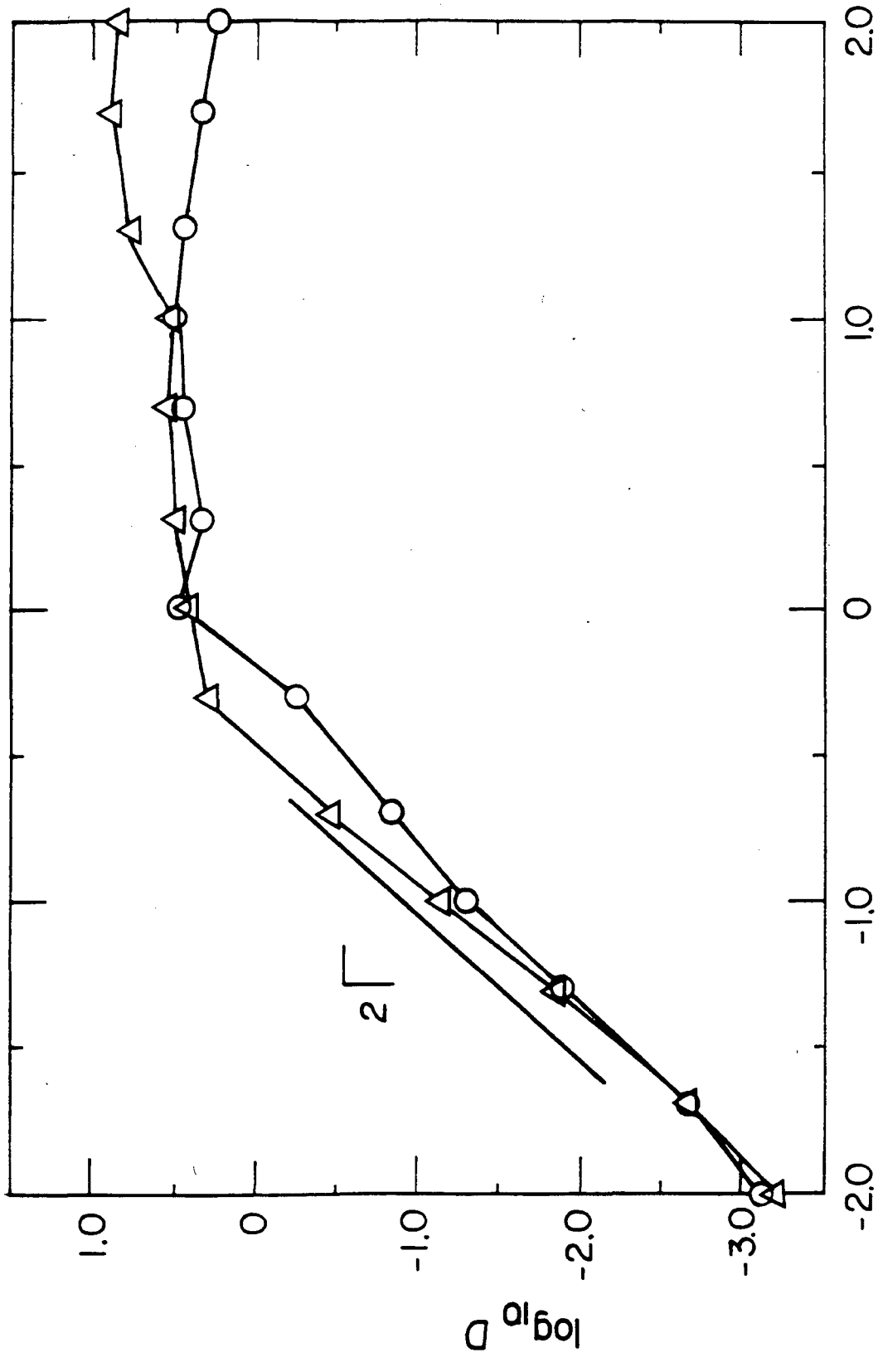

Fig. 4b

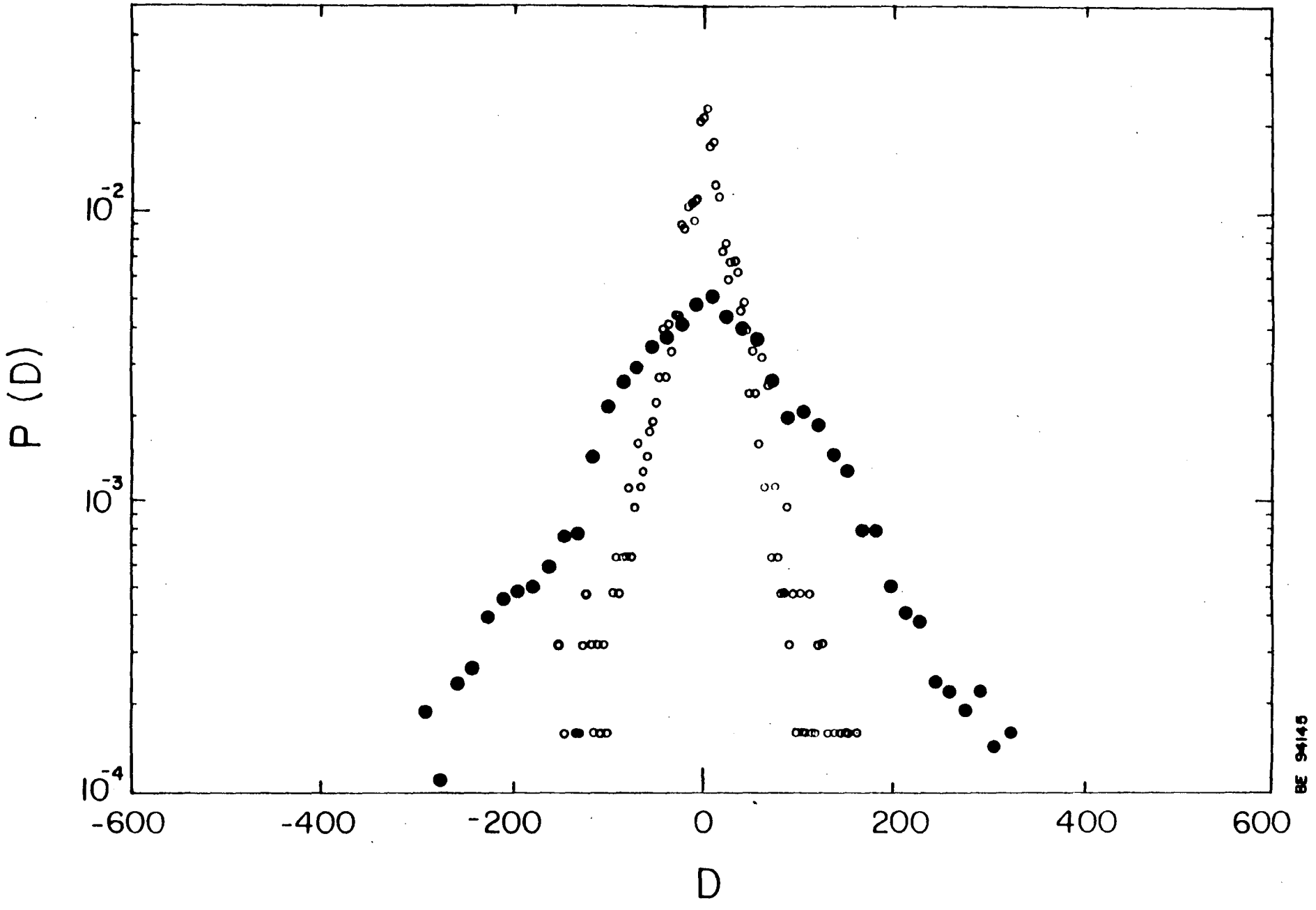

Fig 5a

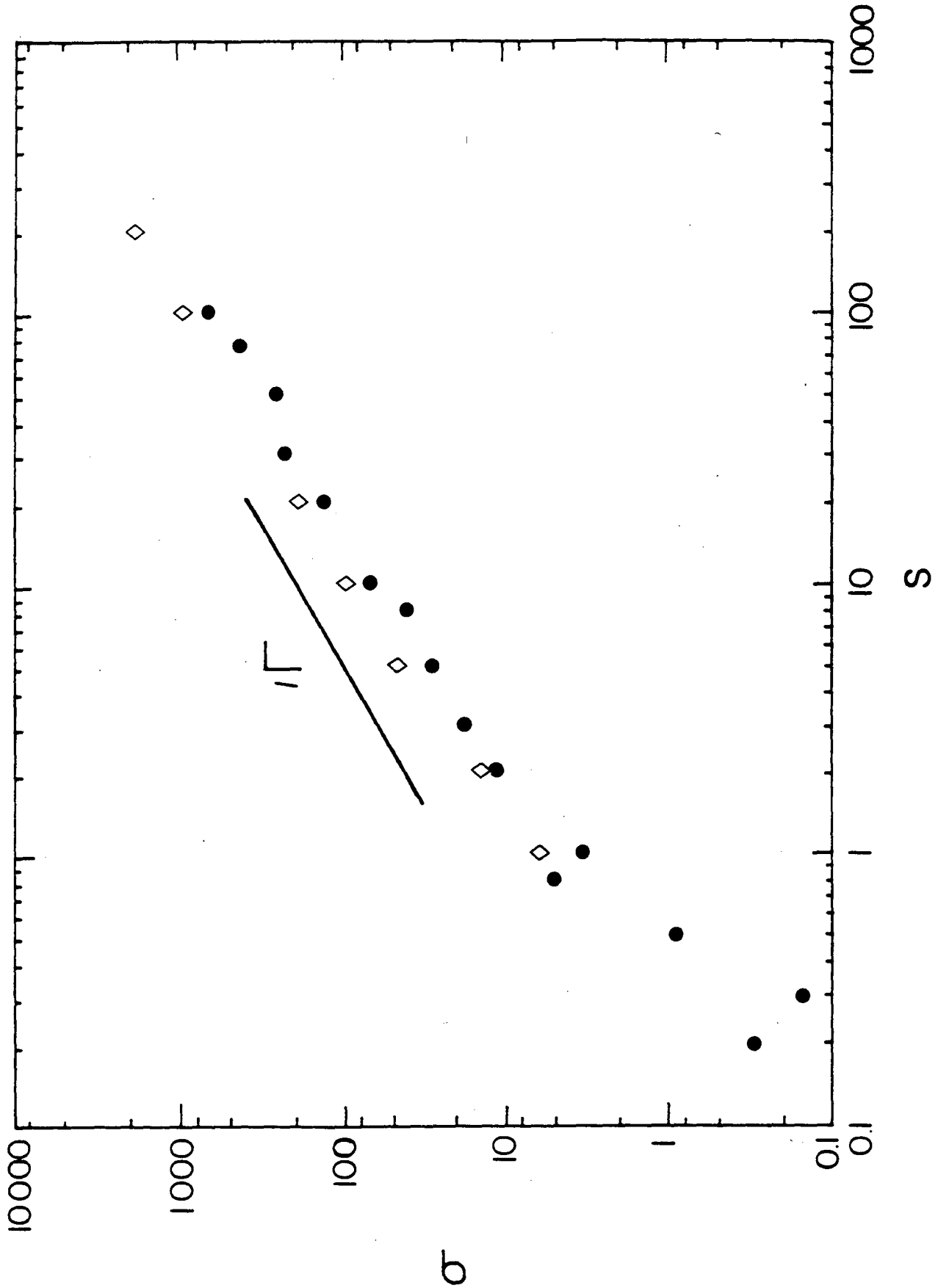

Fig. 5 b

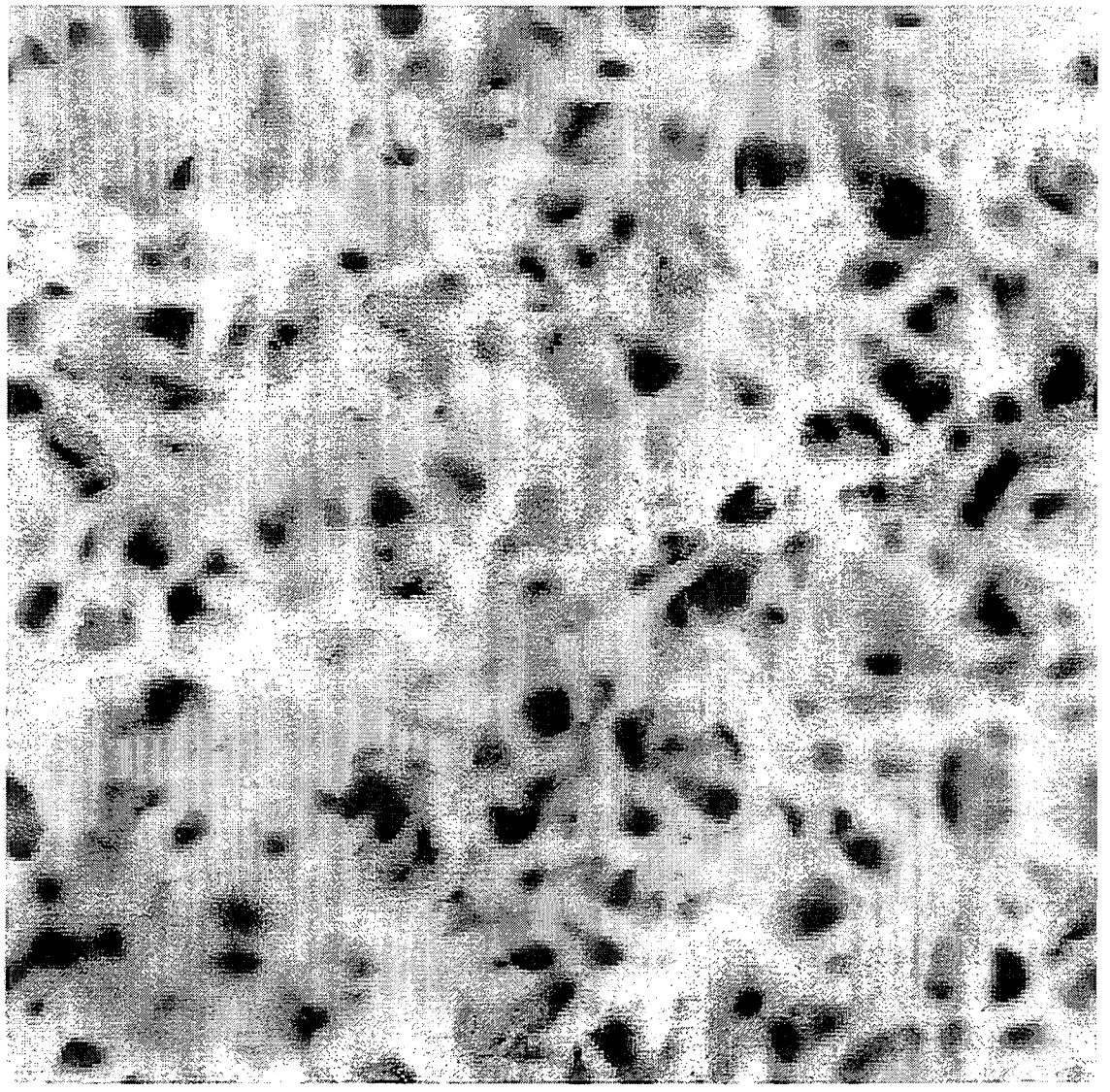

Fig. 6

LAWRENCE BERKELEY LABORATORY
UNIVERSITY OF CALIFORNIA
TECHNICAL INFORMATION DEPARTMENT
BERKELEY, CALIFORNIA 94720